

# Lead pyrovanadate single crystal as a new SRS material

T.T. Basiev, Yu.K. Voron'ko, V.A. Maslov, A.A. Sobol, V.E. Shukshin

**Abstract.** Lead pyrovanadate  $\text{Pb}_2\text{V}_2\text{O}_7$  single crystals of optical quality suitable for laser experiments are obtained. Vibrational modes are identified based on the analysis of the polarised Raman spectra of the single crystals. The main parameters (width at half maximum, peak and integral intensities) of the spectral lines most promising for SRS conversion in this material are estimated. These parameters are compared with the corresponding parameters of the most frequently used lines of known Raman materials: yttrium and gadolinium vanadates, potassium and lead tungstates, and lead molybdate.

**Keywords:** Raman light scattering, lead pyrovanadate  $\text{Pb}_2\text{V}_2\text{O}_7$ , SRS lasers.

## 1. Introduction

The high efficiency of yttrium and gadolinium orthovanadate crystals as SRS-active media was previously demonstrated in [1–5]. It is of interest to evaluate the possibility of SRS conversion in other vanadate crystals, in particular, lead pyrovanadate, which is known as a natural mineral chervetite.

The study of this material also allows one to estimate the effect exerted by the  $\text{Pb}^{2+}$  cation, which has a strong bond covalency, on the cross section of Raman scattering on the internal vibrations of the  $[\text{V}_2\text{O}_7]$  complex. Studying the stimulated Raman scattering in  $\text{MWO}_4$  and  $\text{MMoO}_4$  single crystals of the scheelite structure with  $\text{M} = \text{Ba}, \text{Sr}, \text{Ca},$  and  $\text{Pb}$ , the authors of [6] found that the cross sections of Raman scattering on the internal vibrations of the  $[\text{WO}_4]$  and  $[\text{MoO}_4]$  complexes are anomalously large in the  $\text{PbWO}_4$  and  $\text{PbMoO}_4$  crystals.

In the present work, we comparatively estimate the cross sections of the most intense Raman lines of the internal vibrations of the  $[\text{VO}_4]$ ,  $[\text{V}_2\text{O}_7]$ ,  $[\text{WO}_4]$ , and  $[\text{MoO}_4]$  complexes in the  $\text{Pb}_2\text{V}_2\text{O}_7$ ,  $\text{YVO}_4$ ,  $\text{GdVO}_4$ ,  $\text{PbWO}_4$ ,  $\text{PbMoO}_4$ , and  $\text{CaWO}_4$  single crystals. Since the literature contains no data on the Raman spectra of  $\text{Pb}_2\text{V}_2\text{O}_7$  crystals,

we studied them in polarised light and identified the vibrational spectra.

## 2. Studied crystals and experimental technique

The  $\text{Pb}_2\text{V}_2\text{O}_7$  single crystals were crystallised from a congruent melt [7]. The raw materials ( $\text{PbO}$  and  $\text{V}_2\text{O}_5$ , high purity grade 2–3 for microelectronics) with a total mass of 60 g were melted in a platinum crucible 40 mm in diameter. After homogenisation of the melt at a temperature of 750 °C in a resistance furnace, lead vanadate was spontaneously crystallised on a platinum rod 2 mm in diameter as the melt was cooled with a rate of 0.8 °C h<sup>-1</sup>. The temperature gradient did not exceed 2 °C cm<sup>-1</sup>. To decrease the number of forming centres, the seed holder was pulled with a rate of 5 mm h<sup>-1</sup>. The  $\text{Pb}_2\text{V}_2\text{O}_7$  single crystals had a sheet form and reached dimensions of 3 × 8 × 1 mm.

The size of the single crystals allowed us both to reliably measure the Raman spectra in polarised light and to estimate the scattering cross sections for individual lines. The  $\text{YVO}_4$ ,  $\text{GdVO}_4$ ,  $\text{PbWO}_4$ ,  $\text{PbMoO}_4$ , and  $\text{CaWO}_4$  single crystals studied previously in [1, 6, 8–10] were grown by the Czochralski method. The relative scattering cross sections were measured on identically thick plates under the same conditions of excitation and recording of Raman spectra using the 180° scattering geometry as in works [6, 8, 9]. The spectra were recorded with a SPEX Ramalog 1403 spectrometer with a resolution better than 1 cm<sup>-1</sup> under excitation by the 514.5-nm argon laser line. The line with  $\lambda = 488$  nm was not used due to its strong absorption by the  $\text{Pb}_2\text{V}_2\text{O}_7$  crystal.

## 3. Experimental

According to [11, 12], the  $\text{Pb}_2\text{V}_2\text{O}_7$  crystal structure corresponds to the monoclinic space group  $\text{P2}_1/a$  ( $\text{C}_{2h}^5$ ) with four formula units per unit cell. The structure contains the pyrovanadate anions  $[\text{V}_2\text{O}_7]^{4-}$ . The following atomic positions are identified in the lattice:  $\text{Pb}(1)$ ,  $\text{Pb}(2)$ ,  $\text{V}(1)$ ,  $\text{V}(2)$ , and  $\text{O}(1-7)$ . All the 11 positions have the local symmetry  $\text{C}_1$ . Based on this, we calculated the vibrational spectrum  $\Gamma$  of the crystal for the Brillouin zone centre as

$$\Gamma = 33\text{A}_g + 33\text{B}_g + 33\text{A}_u + 33\text{B}_u.$$

The active vibrations in the Raman spectra are  $33\text{A}_g + 33\text{B}_g$ , and the active vibrations in the IR absorption spectra are  $32\text{A}_u + 31\text{B}_u$ . We managed to separate the  $\text{A}_g$  and  $\text{B}_g$

T.T. Basiev, Yu.K. Voron'ko, V.A. Maslov, A.A. Sobol, V.E. Shukshin  
A.M. Prokhorov General Physics Institute, Russian Academy of Sciences,  
ul. Vavilova 38, 119991 Moscow, Russia;  
e-mail: sobol@lst.gpi.ru, shukshinve@lst.gpi.ru

vibrations using the polarised Raman spectra in different scattering geometries. The Raman tensors for the monoclinic structure have the form

$$\begin{vmatrix} \alpha_{xx} & \cdot & \alpha_{xz} \\ \cdot & \alpha_{yy} & \cdot \\ \alpha_{zx} & \cdot & \alpha_{zz} \end{vmatrix} \quad \text{and} \quad \begin{vmatrix} \cdot & \alpha_{xy} & \cdot \\ \alpha_{yx} & \cdot & \alpha_{yz} \\ \cdot & \alpha_{zy} & \cdot \end{vmatrix}$$

for the  $A_g$  and  $B_g$  vibrations, respectively.

This form of the Raman tensors corresponds to the case when the second-order axis  $C_2$  is parallel to the  $y$  axis of the Cartesian coordinate system and to the crystallographic axis  $b$ . The axes of the single crystal were oriented with respect to the axes of the Cartesian coordinate system as  $a||x$ ,  $b||y$ , and  $c'||z$ . In this case, the  $c'$  axis was perpendicular to the  $ab$  plane. The experiments were performed in the scattering geometries  $x(zz)\bar{x}$ ,  $x(yy)\bar{x}$ , and  $z(xx)\bar{z}$  (in Porto notations) for identification of the  $A_g$  vibrations and in the  $x(yz)\bar{x}$  and  $z(xy)\bar{z}$  geometries for identification of the  $B_g$  vibrations. The choice of these geometries allowed us to avoid the birefringence effects of monoclinic crystals and to maximally separate the  $A_g$  and  $B_g$  vibration lines. The polarised Raman spectra are shown in Fig. 1. The spectra in the region of 20–100  $\text{cm}^{-1}$  are presented in Fig. 2. The results of identification of the symmetry of the observed vibrations are listed in Table 1. We reliably identified 29  $A_g$  vibrations and 8  $B_g$  vibrations. The considerably smaller number of recorded  $B_g$  vibrations compared to the set found from the theoretical group analysis for the  $C_{2h}^5$  structure is explained by the extremely low intensity of most  $B_g$  vibrations. As a result, it

is difficult to separate these lines on the background of intense lines of  $A_g$  vibrations even in polarised spectra. Attention is drawn to the most intense high-frequency  $A_g$  line ( $\Delta\nu = 878 \text{ cm}^{-1}$ ) and to the line with  $\Delta\nu = 579 \text{ cm}^{-1}$  of the same symmetry. According to [13], these lines can be assigned to the symmetric internal vibrations of the end  $\text{VO}_3$  group and of the bridging  $\text{V}-\text{O}-\text{V}$  bond of the pyrovanadate anion, respectively.

**Table 1.** Frequencies and symmetries of vibrations in the lead pyrovanadate crystal at a temperature of 300 K.

Frequency shift/ $\text{cm}^{-1}$		Notations
$A_g$	$B_g$	
34		
	38	
45		
	46	
47		
	53	
57		
61		
74		
	91	
94		
107		
114		
132		
141		
185		
201		
226		
236		
	240	
260		
314		
324		
	335	
352		
360		
369		
373		
387		
579		vibration $\nu_s$ (V–O–V)
678		
	685	
750		
810		line wing
820		
830		line wing
	833	
878		vibration $\nu_s$ ( $\text{VO}_3$ )

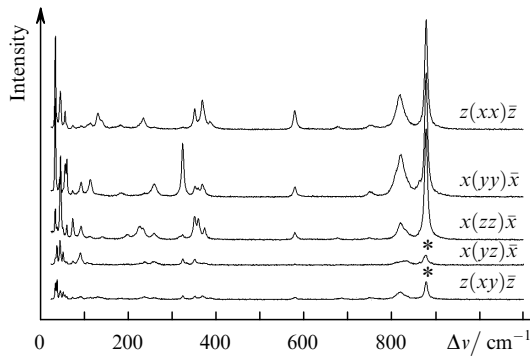


**Figure 1.** Polarised Raman spectra of a lead pyrovanadate single crystal at a temperature of 300 K. The  $A_g$  vibrations are observed in the scattering geometries  $x(zz)\bar{x}$ ,  $x(yy)\bar{x}$ , and  $z(xx)\bar{z}$ , while the  $B_g$  vibrations are observed in the geometries  $x(yz)\bar{x}$  and  $z(xy)\bar{z}$ . The asterisks denote the frequencies of vibrations forbidden in the given scattering geometry.

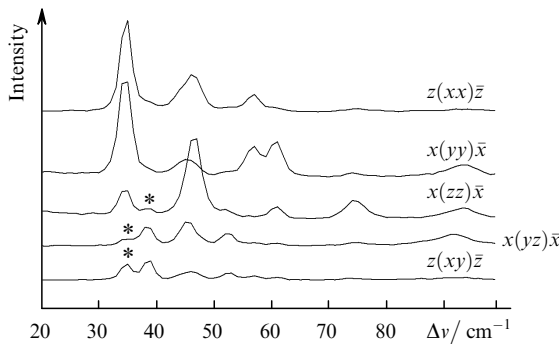


**Figure 2.** Polarised spectra from Fig. 1 in the region of 20–100  $\text{cm}^{-1}$ .

Table 2 lists the spectroscopic parameters of the most intense Raman lines in the studied crystals at a temperature of 300 K. Of particular interest are the line half-widths  $\delta_{1/2}$ , the optical dephasing times  $T_2$ , and the peak ( $\sigma_{\text{peak}}$ ) and integral ( $\sigma_{\text{int}}$ ) line intensities, which allow one to evaluate the potential of the use of materials in Raman lasers [14–19]. One can see that  $\sigma_{\text{int}}$  for the line with  $\Delta\nu = 878 \text{ cm}^{-1}$  of the  $\nu_s$  ( $\text{VO}_3$ ) vibration of the pyrovanadate anion in  $\text{Pb}_2\text{V}_2\text{O}_7$  is higher than for the totally symmetric vibration  $\nu_1$  of the  $[\text{VO}_4]$  tetrahedron in  $\text{GdVO}_4$  (by 30%) and  $\text{YVO}_4$  (by 15%). The small optical dephasing time and the large

linewidth of the  $\nu_s$  ( $\text{VO}_3$ ) vibration ( $8 \text{ cm}^{-1}$ ) compared to the vibration  $\nu_1$  of  $[\text{VO}_4]$  ( $2.6\text{--}2.9 \text{ cm}^{-1}$ ) result in a smaller  $\sigma_{\text{peak}}$  for the studied line in lead pyrovanadate than for the lines  $\nu_1$  in gadolinium and yttrium pyrovanadates, but these parameters are important for realisation of stationary SRS. Table 2 also shows that the integral intensity of Raman lines in vanadate systems increases when the crystal lattice contains the Pb atom as a structural element, although this intensity in the orthomolybdate and orthotungstate structures is even higher. The intensity  $\sigma_{\text{int}}$  for the  $\nu_1$  line in  $\text{PbWO}_4$  and  $\text{PbMoO}_4$  is higher than in  $\text{CaWO}_4$  by a factor of 3.3 and 7.5, respectively (Table 2).

**Table 2.** Spectroscopic parameters of the most intense Raman lines of the studied crystals at 300 K.

Crystal	$\Delta\nu/\text{cm}^{-1}$	$T_2/\text{ps}$	$\delta_{1/2}/\text{cm}^{-1}$	$\sigma_{\text{peak}}$	$\sigma_{\text{int}}$
$\text{PbMoO}_4$	871	1.8	6.0	6.7	7.5
$\text{PbWO}_4$	904	2.6	4.1	5.4	3.3
$\text{Pb}_2\text{V}_2\text{O}_7$	820*	0.5	20.0	0.3	0.7
$\text{Pb}_2\text{V}_2\text{O}_7$	878	1.3	8.0	1.7	2.2
$\text{YVO}_4$	891	4.1	2.6	4.5	1.9
$\text{CaWO}_4$	911	1.8	5.9	1.0	1.0
$\text{GdVO}_4$	884	3.5	3.0	3.9	1.7

Note. Intensities  $\sigma_{\text{peak}}$  and  $\sigma_{\text{int}}$  are normalised to those for the line with  $\Delta\nu = 911 \text{ cm}^{-1}$  in  $\text{CaWO}_4$  and are given for the geometries corresponding to the maximum scattering intensities.

\*Data in this line are given for the total profile with a maximum at  $\Delta\nu = 820 \text{ cm}^{-1}$ .

The large half-widths of the lines of the  $A_g$  symmetry in the Raman spectrum,  $\delta_{1/2} = 8 \text{ cm}^{-1}$  ( $\Delta\nu = 878 \text{ cm}^{-1}$ ) and  $20 \text{ cm}^{-1}$  ( $\Delta\nu = 820 \text{ cm}^{-1}$ ), can be of special interest in quantum electronics for realisation of the stationary SRS and parametric scattering of pico- and subpicosecond laser pulses [14–18].

**Acknowledgements.** This work was supported by the Grant of the President of the Russian Federation for the State Support of Young Russian Scientists (Grant No. MK-816.2010.2).

## References

- Basiev T.T., Zverev P.G., Karasik A.Ya., Vassiliev S.V., Sobol A.A., Chunaev D.S., Konjushkin V.A., Zagumennyi A.I., Zavarstev Y.D., Kutovoi S.A., Osiko V.V., Shcherbakov I.A. *Trends Opt. Photon.*, **94**, 298 (2004).
- Chen Y.F. *Opt. Lett.*, **29**, 2172 (2004).
- Chen Y.F., Ku M.L., Tsai L.Y., Chen Y.C. *Opt. Lett.*, **29**, 2279 (2004).
- Chen Y.F. *Opt. Lett.*, **29**, 2632 (2004).
- Wang B., Tan H., Peng J., Miao J., Gao L. *Opt. Commun.*, **271**, 555 (2007).
- Basiev T.T., Zverev P.G., Karasik A.Ya., Osiko V.V., Sobol A.A., Chunaev D.S. *Zh. Eksp. Teor. Fiz.*, **126**, 1073 (2004).
- Viting L.M., Golubkova G.P. *Vestnik Mosk. Univ. Ser. Khim.*, (3), 88 (1964).
- Basiev T.T., Sobol A.A., Voronko Yu.K., Zverev P.G. *Opt. Mater.*, **15**, 205 (2000).
- Basiev T.T., Sobol A.A., Zverev P.G., Osiko V.V., Powell R.C. *Appl. Opt.*, **38**, 594 (1999).
- Voron'ko Yu.K., Sobol' A.A., Shukshin V.E., Zagumennyi A.I., Zavarstev Yu.D., Kutovoi S.A. *Phys. Solid State*, **51**, 1886 (2009).
- Kawahara A. *Bull. Soc. Fr. Miner. Cristallogr.*, **90**, 279 (1967).
- Shannon R.B., Calvo C. *Can. J. Chem.*, **51**, 70 (1973).
- Voron'ko Yu.K., Sobol A.A., Shukshin V.E. *Neorgan. Mater.*, **41**, 1243 (2005).
- Basiev T.T. *Usp. Fiz. Nauk*, **169**, 1149 (1999).
- Zverev P.G., Basiev T.T., Sobol A.A., Skorniyakov V.V., Ivleva L.I., Polozkov N.M., Osiko V.V. *Kvantovaya Elektron.*, **30** (1), 55 (2000) [*Quantum Electron.*, **30** (1), 55 (2000)].
- Basiev T.T., Powell R.C., in *Handbook of Laser Technology and Applications* (Bristol, Philadelphia: IOP Publ., 2004) Ch. B1.7, p. 469.
- Basiev T.T., Powell R.C. *Opt. Mater.*, **11**, 301 (1999).
- Basiev T.T., Sobol A.A., Zverev P.G., Ivleva L.I., Osiko V.V., Powell R.C. *Opt. Mater.*, **11**, 307 (1999).
- Basiev T.T., Osiko V.V. *Usp. Khim.*, **75**, 1 (2006).